A New Perspective on Airport Delay Prediction: A Three-channel Temporal Convolution Network with Complex Network Information

Shanmei Li, Dengjiang Sun, Chao Wang, Siying Xu, Yang Yang, and Xiaochun Cheng, *Senior Member, IEEE*

***Abstract*—Airport delay prediction plays a crucial role in air traffic management practices, including rerouting aircraft, implementing ground delays, and sequencing arrivals. This task is challenging due to the inherent nonlinear characteristics in traffic evolution. The popular deep learning-based traffic prediction methods lack the in-depth exploration of traffic evolution features. In this work, we propose a novel three-channel Temporal Convolution Network (TCN) framework incorporating temporal complex network feature information for airport delay prediction. The complex network feature sequence of the temporal networks can effectively capture the nonlinear dynamic behavior of airport delays. Firstly, we divide the original time series of airport delays into three distinct series (current, daily, and weekly) and feed them into three channels of our model. This operation allows the model to effectively capture the inherent characteristics of local proximity and global periodicity in airport delay time series. Secondly, the complex networks are converted from airport delay time series using complex network theory, and the topological features of networks are combined with three-chamel TCN, to improve the ability of learning short-term nonlinearity of airport delay evolution. Finally, we incorporate weather condition and flight schedule information as external features to further enhance the prediction accuracy. We perform extensive experiments on a flight dataset at Hartsfield-Jackson Atlanta International Airport (ATL), and the results demonstrate the superiority of our approach compared to existing benchmark methods.**

***Index Terms*—airport delay prediction, deep learning, temporal convolution network, collective cumulative effect, complex network**

I. Introduction

THE rapid expansion of the civil aviation industry has brought attention to the growing disparity between the rising demand for air traffic and the constrained capacity, leading to notable flight delays. Based on data from 2019, the average flight delay in Europe, the United States, and China was 13.1 minutes, 12.9 minutes, and 14 minutes, respectively [1]–[3]. At present, airport delays are increasingly viewed as indicators of the efficiency of air traffic management. Accurate prediction of airport delays plays a crucial role in optimizing flights, airports, and airspace resources. It also provides vital support for the automation of air traffic management.

Predicting airport delays is a highly challenging task due to two types of complex factors: transmission factors and original factors. Transmission factors refer to significant flight delays experienced in upstream airports, while original factors encompass human error, adverse weather conditions, mechanical failures, military activities, and other similar factors [4]. These factors are interconnected and interdependent, resulting in the complex spatiotemporal evolution of airport delays. Consequently, developing an effective mathematical model that accurately represents these intricate relationships is no easy task.

The increasing availability of flight operation data and advancements in artificial intelligence technology present opportunities for data-driven airport delay prediction. Previous studies have mainly focused on forecasting the delays of individual flights within specific areas, such as airports, sectors, or terminals [5], [6]. However, air traffic managers often require an understanding of the overall extent of delays that will occur in the future, rather than solely focusing on individual flight situations. Therefore, our approach directly predicts airport delays.

To examine the dynamic nature of airport delays, we demonstrate the time series of the average flight delay at Hartsfield-Jackson International Airport in Atlanta, United States. Figure 1(a) illustrates the overall trend of average flight delay over one week, while Figure 1(b) displays the delays specifically on weekdays from 5:00 to 21:00. These figures reveal three distinct patterns in the evolution of airport delays.

1. **Local proximity**. The airport delay in the later interval is greatly affected by the delay in the previous interval. The correlation between different time intervals diminishes as the temporal distance increases. For instance, the delay conditions at 8 pm might be influenced by the airport delay appearing at 7 pm, but is less affected by the delay at 5 am of the same day.

2. **Global periodicity**. The average departure delay on different weekdays exhibits temporal periodicity, encompassing both daily and weekly patterns. Delays experienced at the same time intervals, such as during afternoon rush hours, tend to be

This work is supported by the National Natural Science Foundation of China under Grant No. 71801215, the Key Program of Tianjin Science and Technology Plan under Grant No.21JCZDJC00840 and 21JCZDJC00780, the Fundamental Research Funds for the Central Universities under Grant No. 312202YY02 and 3122018D026, and the Civil Aviation Administration of China Safety Capacity Building Fund under Grant No.SKZ49420220027. (*Corresponding author: Xiaochun Cheng*).

Shanmei Li, Chao Wang, and Yang Yang are with the College of Air Traffic Management, Civil Aviation University of China, Tianjin 300300, China. E-mail: sm-li@cauc.edu.cn, chaowang@cauc.edu.cn, 1833367807@qq.com

Xiaochun Cheng is affliated with the Department of Computer Science, Swansea University, Swansea SA1 8EN, UK. E-mail: Xiaochun.Cheng@Swansea.ac.uk.

Siying Xu is with the Operation Supervisory Centre, Civil Aviation Administration of China, Beijing 100710, China. E-mail: siyingxu2001@163.com

Dengjiang Sun is with the School of Systems Science, Beijing Jiaotong University, Beijing 100044, China. E-mail: dj-sun@bjtu.edu.cn

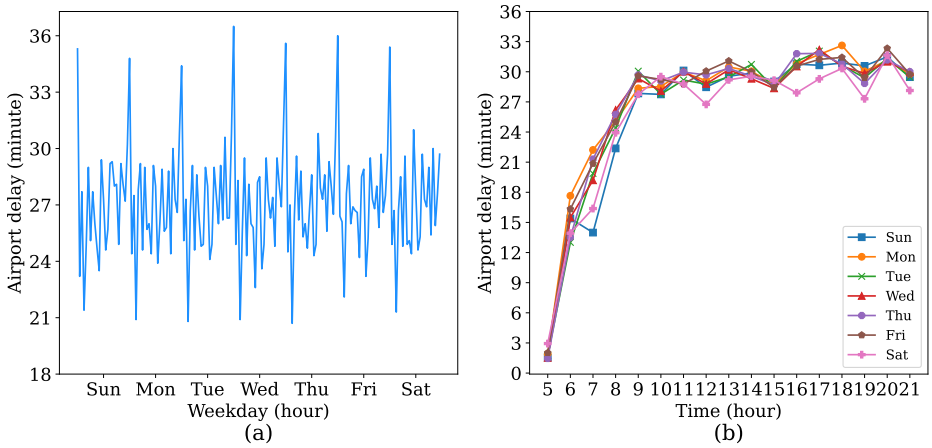

Fig. 1. Examples of airport delay. (a) Airport delay of ATL during one week. (b) Airport delay of ATL from 5:00 am to 21:00 pm.

consistent on consecutive weekdays. Furthermore, an analysis of eight weeks' delay data unveils similarities between the delays observed on a specific weekday and the corresponding days in other weeks.

3. **Short-term nonlinearity**. The nonlinearity of airport delays comes from multiple uncertain factors, including weather conditions, equipment failures, and more. Smaller time intervals exhibit higher volatility in airport delays, while different time intervals display distinct fluctuation patterns. Therefore, quantifying these nonlinear characteristics can contribute to enhancing prediction accuracy.

The local proximity and periodicity characteristics suggest that airport delays within a given time interval are influenced by delays in neighboring intervals on the same day and those in previous days. Similarly, these features are also present in ground traffic. Chen et al. developed a deep learning traffic congestion prediction model that considers these two features, achieving good predictive performance [7]. The nonlinearity observed in airport delay time series constitutes a crucial factor affecting prediction accuracy. To the best of our knowledge, the short-term nonlinearity indicators in airport delays have not yet been incorporated into airport delay prediction models. The primary issue that needs to be addressed is how to measure this nonlinearity.

Complex network theory has become an important tool for characterizing complex systems. Its fundamental premise is to map a real-world system to a network, where nodes represent the system's components and edges describe the relationships among these components [8]. Holme et al. have proposed that the network structure aids in understanding, predicting, and optimizing the behavior of dynamical systems [9]. In particular, complex network theory can effectively extract topological characteristics from time series. Lacasa et al. (2008) and Luque et al. (2009) introduced the visibility graph (VG) and horizontal visibility graph (HVG), which facilitate the rapid and straightforward mapping of time series to complex networks [10], [11]. Gao et al. (2016) developed the limited penetrable visibility graph (LPVG) for analyzing nonlinear time series [12]. The LPVG exhibits excellent noise resistance, allowing for the extraction of nonlinear features underlying experimental measurements. Consequently, the topology features of complex networks can be applied to discern nonlinearity in time series.

Moreover, environmental factors, specifically weather conditions, along with the schedule traffic flow, are two essential factors contributing to flight delays. Therefore, it is imperative for airport delay prediction models to consider weather variables and schedule traffic flow.

To capture the similar patterns and nonlinear properties of airport delays, we propose a Temporal Convolution Networks (TCN) based airport Delay Prediction considering local Proximity, global Periodicity and short-term Nonlinearity (TDP-PPN). The TDP-PPN model primarily comprises three essential procedures: a complex network module, a mutifeature learning module and an attention mechanism module. By applying the time series of airport delays to the three-channel TCN, TDP-PPN can effectively capture the inherent characteristics of local proximity, global periodicity, and short-term nonlinearity.

Our experiment is implemented using the real flight records data at U.S. ATL airport. We evaluate the performance of TDP-PPN by comparing it with baseline time series prediction methods. The experimental results indicate that TDP-PPN achieves significantly higher prediction accuracy. Furthermore, we also compare different variations of TDP-PPN to showcase its exceptional performance.

The main contributions of this paper can be summarized as follows:

- We propose a novel complex network-based deep learning method for airport delay prediction. Time series of three indicators related to airport delays are mapped to temporal networks based on LPVG, and the degree centrality and clustering coefficient sequences of networks represent the delay behavior characterization. By examining the distribution of degree centrality and clustering coefficient, we explore the nonlinear mechanisms underlying airport delays. To the best of our knowledge, this study represents the first time of combining complex

network topology features with deep learning in the context of airport delay prediction research.
- A three-channel Temporal Convolutional Network (TCN) model for airport delay prediction is developed. This model incorporates three channels to model local temporal dependencies, global periodic patterns, and short-term nonlinearity, effectively capturing immediate past information, similar historical patterns, and nonlinear behavior concurrently. Furthermore, the model accounts for flight schedules and weather conditions, which are crucial factors affecting airport delays.
- The experimental prediction results reveal that the combined utilization of current situations, day/week based periodic patterns, and nonlinearity can significantly enhance the accuracy of predictions.

The remainder of this paper is structured as follows: Section II provides a review of studies concerning flight delay prediction. Section III presents the airport delay indicators. The TDP-PPN model for airport delay prediction is presented in Section IV. Section V discusses the experimental results. Lastly, Section VI presents the conclusion.

II. Literature Review

Air traffic delay prediction is a crucial application in intelligent air transportation systems (IATS). Thus far, extensive efforts have been dedicated to the exploration of airport delay prediction, which can be broadly categorized into three main areas: statistical inference methods, simulation modeling methods, and machine learning methods.

A. Statistical inference methods

Statistical inference methods analyze the characteristics of the sample data, primarily historical data, and construct empirical or theoretical statistical models to estimate quantitative characteristics of the overall data and predict airport delays. Tu et al. developed a probability model that accounts for daily and seasonal trends [13]. Mueller and Chatterji found that departure delays follow a Poisson distribution, while enroute and arrival delays adhere to a normal distribution [14]. Boswell et al. employed probability density functions to express delay categories [15]. Wong and Tsai established a Cox proportional hazards model for flight delay prediction based on survival analysis [16].

B. Simulation modeling methods

Simulation modeling methods employ computers to simulate flight operation models, including aircraft operation models, delay propagation models, and more. Hansen et al. developed a straightforward deterministic queuing model to analyze the externalities of runway delay [17]. Pyrgiotis et al. utilized queuing models to examine delay propagation among different airports [18]. Pablo Fleurquin constructed an agent-based model to identify delay propagation patterns [19]. Baspinar et al. constructed two distinct data-driven epidemic models to simulate the propagation of air transportation delays [20].

C. Machine learning methods

Machine learning models for flight delay prediction aim to identify crucial factors that contribute to flight delays by analyzing vast quantities of flight data. With the increasing convenience of data acquisition, machine learning and deep learning-based flight delay prediction become popular [21], [22]. Rodríguez-Sanz et al. developed a Bayesian network arrival delay prediction model [23]. Gui et al. built a classification and regression model for individual flight delays based on random forest algorithm, and the model took account of multi-source information (e.g., meteorological conditions, flight schedules, airport information) [24]. Kim et al. proposed a long short-term memory (LSTM) architecture for predicting classified flight delays [25]. Zeng et al. developed a deep graph neural network-based delay prediction model [26].

This paper focuses on utilizing deep learning techniques for accurately predicting short-term airport delays. Unlike previous studies, we simultaneously consider the features of periodicity, local proximity, and nonlinearity, which have rarely been examined together.

III. Preliminaries

In general, flight delay is determined by the disparity between the scheduled and actual departure or arrival times. As per the guidelines set by the Federal Aviation Administration (FAA), a flight is classified as delayed if its delay exceeds 15 minutes. It's important to note that the delay status of an airport is not specific to a single flight, but rather pertains to the collective delay situation of the group of flights departing and arriving within a given time interval. As the delay of arrival flights may not occur in the airport but at the air route, we use the delay of departure flights to evaluate the airport delay.

Definition 1 (Flight Delay)**.** The delay of the k_{th} flight in time interval j of day i,$P_{i,j,k}$, is defined as the difference between the real and the scheduled departure time $(T^r_{i,j,k}, T^s_{i,j,k})$. If the difference is negative, $P_{i,j,k}$ would be defined as 0. Thus,

$$P_{i,j,k} = \max(T^r_{i,j,k} - T^s_{i,j,k}, 0) \tag{1}$$

Definition 2 (Departure Traffic Flow)**.** The departure traffic flow refers to the quantity of flights departing from an airport. Higher traffic flow typically results in increased airport delays. Departure Traffic Flow (DTF):

$$DTF_{i,j} = Z_{i,j} \tag{2}$$

where $Z_{i,j}$ is the number of departure flights in time interval j of day i .

Definition 3 (Airport Delay)**.** In our study, we consider the average departure delay and departure delay rate as indicators of airport delays. These metrics are commonly used in the operational practices of the civil aviation industry.

- Average Departure Delay (ADD):

$$ADD_{i,j} = \frac{1}{Z_{i,j}} \sum_{k=1}^{Z_{i,j}} P_{i,j,k} \tag{3}$$

- Flight Delay Rate (FDR):

$$FDR_{i,j} = \frac{H_{i,j}}{\mathrm{Z}_{i,j}} \tag{4}$$

$$H_{i,j} = \sum_{k=1}^{z_{i,j}} \gamma_{i,j,k}, \gamma_{i,j,k} = \begin{cases} 1, & P_{i,j,k} \geq 15min \\ 0, & P_{i,j,k} < 15min \end{cases} \tag{5}$$

where $H_{i,j}$is the number of delayed flights in time interval j of day i. The k_{th} flight is considered as a delayed flight if $P_{i,j,k} \geq 15min$.

IV. Methodology

In this section, we begin by describing the architecture of the proposed model for predicting airport delays. Subsequently, we provide a detailed explanation of each component of the model.

A. Overview

In this paper, we propose a model called TDP-PPN to capture the features of local proximity, global periodicity, and nonlinearity for predicting short-term airport delays. The architecture of TDP-PPN is shown in Figure 2 and consists of three main modules: the complex network module, the multi-feature learning module, and the attention mechanism module. To begin, as depicted in the left portion of Figure 2, we consider time intervals of 5 minutes, resulting in a total of 288 intervals in a day for the raw input data. Initially, we utilize historical data from the previous p days to generate time series for ADD, FDR, and DTF. These time series are then separately inputted into the complex network construction module and the multi-feature learning module. The complex network construction module constructs complex networks using the ADD, DTF and FDR time series and calculates their corresponding network characteristics. Subsequently, the time series of network characteristics, along with the ADD, FDR, and DTF time series, are fed into the multi-feature learning module which utilizes three-channel TCN to capture current, periodic, and nonlinear features. Finally, the output of the TCNs, along with the time series of scheduled traffic flow and weather indicators, are transmitted to the attention mechanism module to obtain the predicted values.

B. Complex network module

To investigate the nonlinearity within the time series of airport delay indicators, we utilize LPVG to transform the time series of airport delays into complex networks. The LPVG method is an enhancement of the VG algorithm, which improves upon the original by mapping a time series onto a graph that preserves the temporal characteristics of the series. This approach enables the detection of not only the distinction between random and chaotic series but also the identification of the spatial locations of inverse bifurcations within chaotic dynamical systems. Furthermore, LPVG exhibits a notable advantage over VG, demonstrating robust performance even in the presence of noise interference.

We initially employ a sliding window approach to divide the ADD, FDR, and DTF time series into subsequences with a 5-minute interval. Given a sliding window of 1 hour, we obtain hourly ADD, FDR, and DTF subsequences, each with a length of 12. Subsequently, we convert these hourly subsequences into complex networks using the LPVG algorithm. The resulting topological feature sequence of the temporal networks effectively captures the nonlinear dynamic behavior of airport delays. The methodology is illustrated in Figure 3 (a).

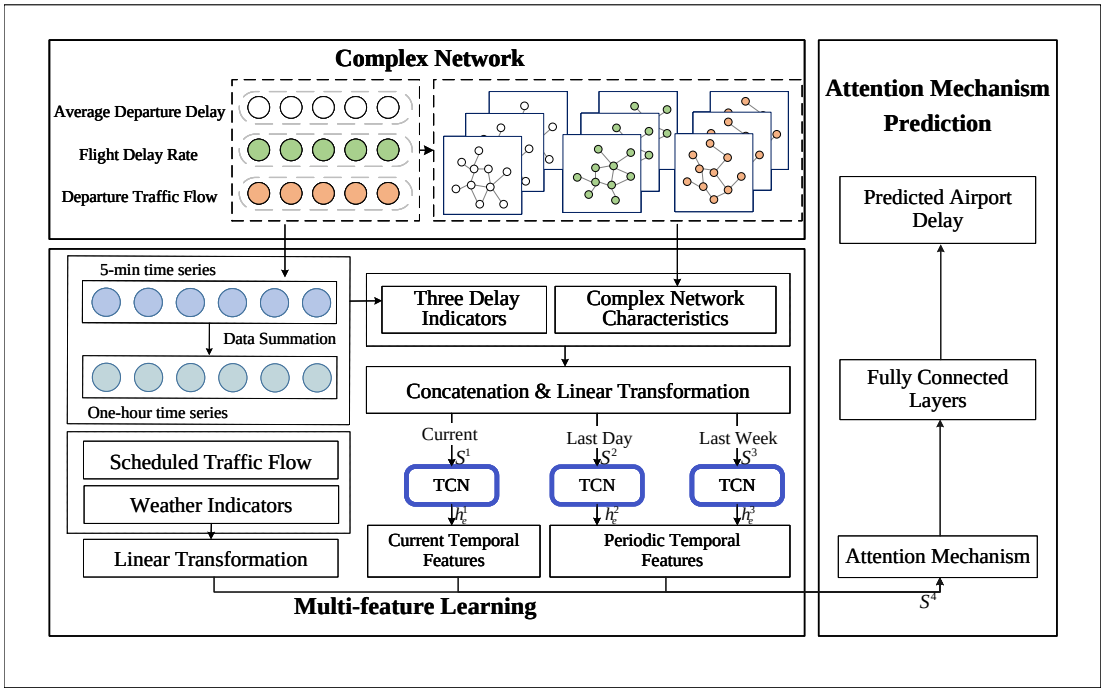

Fig. 2. Architecture of TDP-PPN

In the LPVG algorithm, each point in time series is considered as a node of the network. There is an edge connecting two nodes if they are visible to each other. There is a critical parameter, i.e., limited penetrable distance N, determining whether two points are visible. Consider traffic time series $y(t_1), y(t_2), \ldots, y(t_n)$, two nodes $(t_a, y(t_a))$ and $(t_b, y(t_b))$ with m nodes between them are visible, if there are k $(k \leq N)$ nodes $(t_i, y(t_i)), t_a < t_i < t_b$ fulfill,

$$y(t_i) > y(t_b) + (y(t_a) - y(t_b))\frac{t_b - t_i}{t_b - t_a} \tag{6}$$

And the other $m - k$ nodes $(t_j, y(t_j))$ fulfill,

$$y(t_j) < y(t_b) + (y(t_a) - y(t_b))\frac{t_b - t_j}{t_b - t_a} \tag{7}$$

Figure 3 (b) exemplifies the conversion of hourly subsequences into a network. To illustrate this process, we consider ADD as an example. We initially represent the points of the time series as vertical bars, with the height of each bar corresponding to the value of the time point and its position identical to that in the time series, as depicted in Figure 3 (b). Next, we connect every pair of bars if the line of sight between them is not obstructed (indicated by solid lines), or if the obstruction is limited to a single bar (the maximum penetrable distance is set to 1 in our study), as shown by dashed lines. The corresponding adjacency matrix and network structure are then obtained, as illustrated in Figure 3 (b). Since we construct three networks for each hour based on ADD, FDR, and DTF subsequences, it is necessary to integrate these networks into a single network. We achieve this by performing a logical OR operation on the three matrices of ADD, FDR, and DTF. Consequently, for two nodes to be connected by a line, they must be interconnected in one of the three networks.

Complex networks possess various topological characteristics, including node degree, clustering coefficient, and average path length. In this study, we employ degree centrality and clustering coefficient as metrics to quantify the nonlinearity within the time series.

1) Degree centrality: Degree centrality quantifies the proximity of each node to the center of the network. The center of the network corresponds to the node with the highest degree, which is determined by the number of edges connecting to it.

$$D(i) = \frac{K(i)}{Q-1}, K(i) = \sum_{j=1}^{Q} a_{ij} \tag{8}$$

Here, $a_{ij} = 1$ means there is an edge connecting node i and node j, otherwise, $a_{ij} = 0$. $D(i)$ is the degree centrality of node i. Q is the number of nodes in the network and $K(i)$ is the degree of node i.

2) Clustering coefficient: The clustering coefficient measures the cliquishness of a node in a network. It is calculated as the average clustering coefficient for all nodes in the network.

$$C(i) = \frac{2E(i)}{K(i)(K(i)-1)} \tag{9}$$

where $E(i)$ is the number of edges between the neighbors of node i. $C(i)$ is the clustering coefficient of node i.

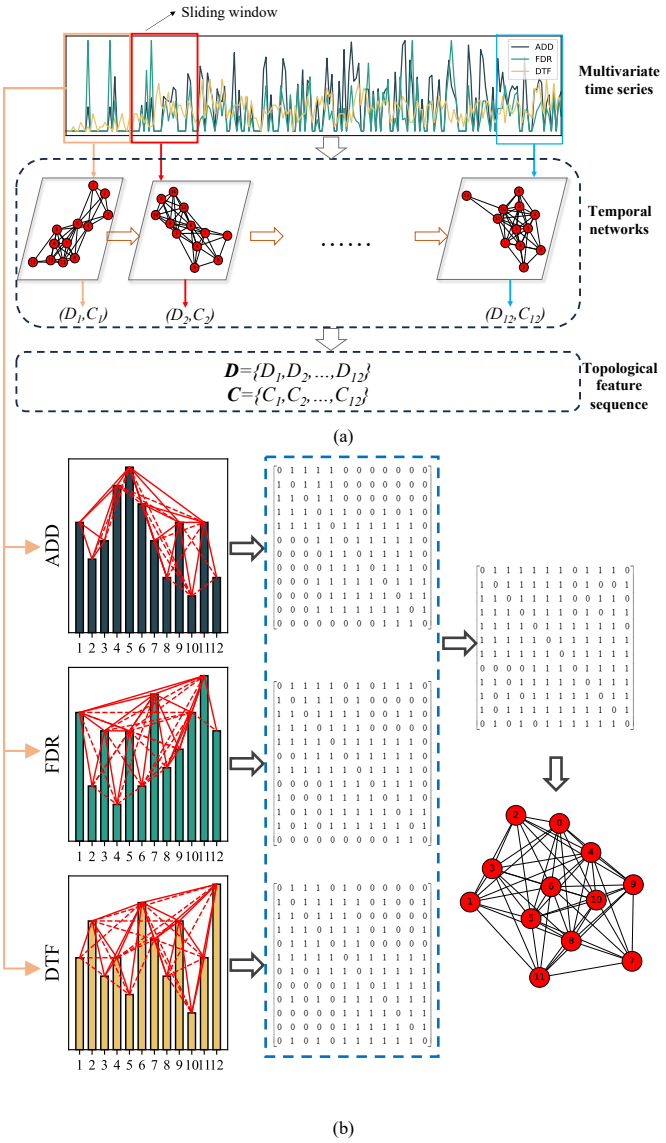

Fig. 3. Schematic diagram of mapping time series to networks

C. Multi-feature learning module

The multi-feature learning module takes several inputs, including time series data of ADD, FDR, DTF, degree centrality, and clustering coefficient. They are concatenated and transformed into a higher dimensional sequence, denoted as S^1. For daily features, we extract a sequence S^2 from S^1 within the same time interval as the near dependencies observed on the previous day. For weekly features, we extract a sequence S^3 in the designated time interval on the same weekday. For example, if we want to predict the delay indicators at time interval t, we have to separately use data from $t - m - 24$ to $t - 1 - 24$ intervals and data from $t - m - 7 \times 24$ to $t - 1 - 7 \times 24$ intervals to capture periodic features, where m denotes the length of data slice. S^1,S^2,S^3 are the inputs of each channel, respectively. Consequently, the model can effectively capture the local proximity, global periodicity, and short-term nonlinearity within the airport delay time series

simultaneously.

The TCN algorithm is a novel approach for time-series prediction and has been successfully applied in various domains such as electroencephalogram [27] and wind power [28]. TCN employs causal convolution to ensure that the prediction at time step $t+1$ is only influenced by the preceding t time steps. Additionally, the use of dilated convolution allows for processing input data in jumps, thereby expanding the network's receptive field without increasing the depth. This paper firstly employees TCN network for the task of airport delay prediction.

The proposed TCN comprises E convolutional layers. The first layer is a causal convolution, followed by an $E-1$ dilated convolution layers. The architecture of the TCN applied in the proposed model is illustrated in Figure 4. In the e_{th} convolutional layer, the kernel size is K, and the dilation factor is $d = K^{e-1}$.

Firstly, the sequences S^1,S^2,$S^3$are utilized as the input to TCN-1, TCN-2, and TCN-3. Specifically, considering the $i-step$ operation of $S^n = (s_1^n, s_2^n, \cdots, s_t^n)$,$(n = 1, 2, 3)$ in the first causal convolutional layer, the detailed operation of the first causal convolution is as follows:

$$h_1^n[i] = f(\sum_{k=1}^{K} W_1[k] s_{i+k-1}^n + b_1) \tag{10}$$

where $W_1[k]$ is the matrix composed of the elements in the k_{th} row of the convolution kernel W_1, $b_1$is bias,$f(\cdot)$is activation function, and h_1^n represents the operation result. The hidden feature matrix of the first layer is denoted as

$$H^{(1)} = (h_1^1, h_1^2, h_1^3)^T \tag{11}$$

After the first causal convolution, the hidden features of S^1,S^2,S^3 undergo $(E-1)$ dilated convolutional layers. Specifically, considering the $i-step$ operation of the S^n hidden feature in the e_{th} th convolutional layer as an example, the operation process of dilated convolution is as follows:

$$h_e^n[i] = f(\sum_{k=1}^{K} W_e[k] h_{e-1}^n[i + (k-1) \times d_e] + b_e) \tag{12}$$

where W_e and b_e represent the kernel and bias term of the e_{th} convolutional layer. $h_{e-1}^n[i + (k-1) \times d_e]$ and $h_e^n[i]$ are the input term and output term of the i_{th}th step operation of S^n.

Through the above operation, the hidden feature vector h_e^n of S^n after the e_{th} th convolution is obtained, which is denoted as

$$H^{(e)} = (h_e^1, h_e^2, h_e^3)^T \tag{13}$$

The temporal convolutional layers are organized into blocks, interconnected by residual connections. Each residual block comprises two dilated convolution layers, followed by a rectified linear unit (ReLU) activation function. Furthermore, the TCN incorporates regularization through dropout applied to each residual block after the dilation convolution layers. The architecture of the residual block is depicted in Figure 4.

It is noted that the flight plan and weather conditions are two important factors influencing airport delay. Thus, the scheduled departure traffic flow and important weather indicators are considered in the prediction model. To enhance the model's performance, the output of the three channels, along with the scheduled departure traffic flow and important weather indicators, will be concatenated and transformed into a higher dimensional representation denoted as S^4 .

D. Attention mechanism module

The temporal attention mechanism allows for the weighting of hidden states across different time dimensions, thereby enhancing the model's sensitivity to dynamic features in the temporal dimension. This effectively improves the model's performance in extracting time-based features. The attention mechanism is represented by:

$$\begin{aligned} V_{(F\times T)} &= (S_t^4)^T W_t + b \\ B_{(F\times T)} &= \frac{\exp(V_{ij})}{\sum_{t-T}^{t}(V_{ij})}, i \in [1, F] \\ \beta &= \frac{\sum_{m=1}^{F} B_{mn}}{F} = [\beta_{t-T}, \beta_{t-T+1}, \cdots, \beta_{t-1}] \end{aligned} \tag{14}$$

where V is the non-normalized probability weight matrix obtained by the inversion of the input matrix S_t^4. W_t is the

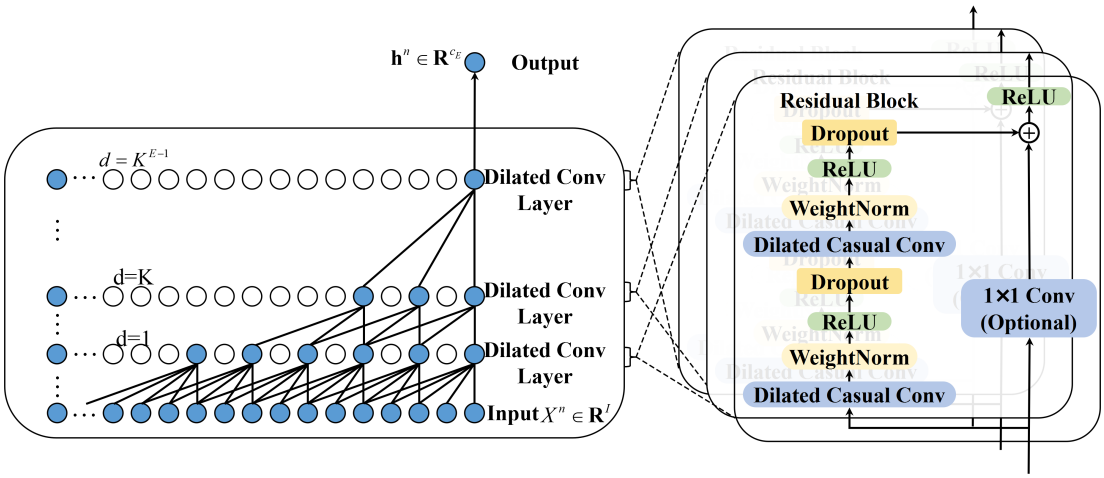

Fig. 4. Architecture of TCN

TABLE I
FLIGHT DATA FORMAT

Flight date	Origin airport	Destination airport	Scheduled departure time	Actual departure time	Scheduled arrival time	Actual arrival time
2019/1/1	ATL	FLL	1000	955	1155	1143
2019/1/8	ATL	TTN	755	746	1002	946
2019/1/17	ATL	DEN	2005	2001	2137	2147
2019/1/24	ATL	EWR	1245	1637	1500	1855
2019/1/27	ATL	IAD	1425	1419	1606	1557
...	...	...	...	...	...	...

weight matrix of the neural network. b is the offset vector. B is the probability weight matrix after the normalization operation, and the sum of probability weights in each row of the matrix is 1. β is the final attention vector.

Finally, the weighted hidden state, the original hidden state, and the auxiliary features are passed through a fully connected layer to generate the final prediction results.

V. EXPERIMENTS AND RESULTS

The dataset utilized in this paper was provided by the U.S. Department of Transportation. It consists of all domestic flights arriving at or departing from ATL between 5 am and 10 pm from January 1st to December 31st, 2019. Each flight record includes details such as the flight date, real and scheduled departure (arrival) times, as well as the origin and destination airports. Records with missing values were treated as outliers and subsequently removed. To facilitate readers' understanding of the data format, Table I presents the original information of some flights. And then, we applied the calculation formulas for ADD, FDR, and DTF, as provided in the "Preliminaries" section, to the original flight data to compute the time series values of these indicators at 5-minute and 1-hour intervals, respectively. Due to space limitations, Figure 5 presents the calculation results of the airport delay indicators for one week. To standardize the data within the range of [0, 1], we apply the max-min normalization method.

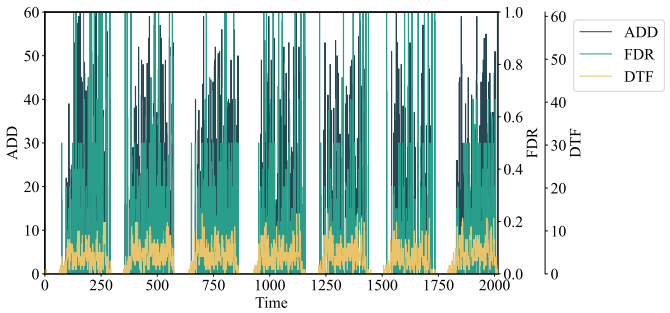

Fig. 5. Airport delay indicators for one week

The meteorological observation data for ATL in 2019 were obtained from the website of the National Oceanic and Atmospheric Administration (NOAA) of the United States. In this study, wind speed, wind direction, precipitation and relative humidity are chosen for the delay prediction.

The explanation of the meteorological data is as follows:

- Wind speed: the hourly average wind speed of airports, and the unit is km/h.
- Wind direction: the hourly average wind direction of airports.
- Precipitation: the hourly average precipitation of airports, and the unit is mm.
- Relative humidity: the average relative humidity of the airport in each hour.

A. Airport delay analysis

To gain a better understanding of the airport delay data, we analyze the frequency distribution of ADD as depicted in Figure 6. It is worth noting that flights with delays exceeding 100 minutes constitute 2.375% of the total, and are considered abnormal in this study. Evidently, the distribution of airport delay exhibits a right-skewed pattern.

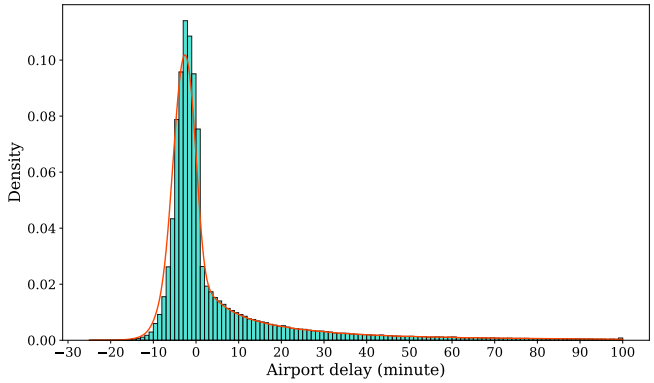

Fig. 6. The frequency distribution of average departure delay

B. Weather analysis

Weather conditions have a substantial impact on airport delays, with longer average delays occurring during severe weather events. Figure 7 illustrates the measurement of weather's influence on airport delays using four indicators: wind speed, wind direction, precipitation, and relative humidity. Each weather indicator is categorized into six levels, ranging from low to high. The distributions of airport delays vary across different weather levels, as indicated by differences in median and box length. Therefore, it can be inferred that there exist relationships between airport delays and weather indicators.

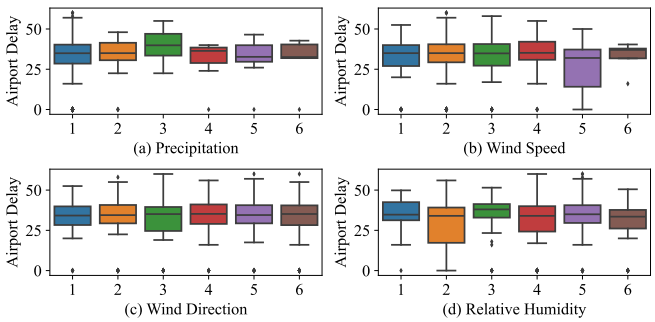

Fig. 7. The distribution of airport delay under different weather levels

C. Complex network analysis

The LPVG algorithm, discussed in Section IV-B, is employed to construct a total of 6205 networks. To assess the variation in network structure across different airport delays, key statistical characteristics such as degree centrality and clustering coefficient are computed for each constructed networks.

Figure 8 presents the calculated results of degree centrality and clustering coefficient for 120 networks. These two characteristics display a notable periodicity, with a cycle consisting of 17 samples. This cycle aligns with the number of samples considered for each day in this study, which is 17 (from 5 am to 10 pm). Thus, we can deduce that the network characteristics undergo a one-day cycle.

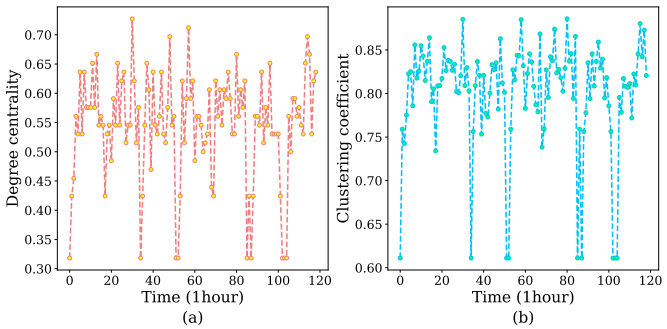

Fig. 8. Examples of complex network characteristics. (a) degree centrality, (b) clustering coefficient

To better understand the relationship between degree centrality (clustering coefficient) and airport delays, the distribution of degree centrality and clustering coefficient under different delay levels and their box plots are shown in Figure 9. Here, slight delay represents ADD $\leq$ 20min, moderate delay represents 20 min $<$ ADD $<$ 40 min, and serious delay represents ADD $\geq$ 40 min. It can be found that serious delay usually has much higher degree centrality and clustering coefficient, and slight delay has much smaller degree centrality and clustering coefficient. Thus, complex network features have some relationship with airport delays. Our method can effectively characterize the complicated airport delay behavior and reveal the evolution from slight delay to heavy delay.

D. Airport delay prediction results

To assess the performance and effectiveness of the TDP-PPN model, we utilize the processed dataset detailed in this section. This dataset encompasses various fundamental airport delay properties, complex network characteristics, schedule traffic flow and weather indicators. We train the TDP-PPN model with different hyperparameter, identifying the set of hyperparameter that yield the optimal results. Additionally, we conduct a comparative analysis of the TDP-PPN model with other baseline models and present the results of this comparison.

1) Hyperparameter: The hidden layer dimension, batch size and input step size of TCN in TDP-PPN model are determined through multiple trial calculations. For the dataset used in this paper, the prediction performance reaches the best when the dimension of hidden layer, the batch size and the optimal input step are set as 64, 64 and 6, separately. Parameters in TCN such as the convolution kernel size K is set to 3, the hidden layers number E is set to 3, the dilated factors d are set to 1, 3, 9. The ReLU activation function are employed in TDP-PPN model. The mean absolute error (MAE) is chosen as the Loss Function. The optimizer is Adam, and the learning rate is set as 1e-3. The dataset is divided into three subsets: 70% for training, 15% for testing, and the remaining 15% for validation.

2) Evaluation metrics: To evaluate the performance of TDP-PPN, the mean absolute error (MAE) and the root-mean-square error (RMSE) are employed.

$$MAE = \frac{1}{M \times N} \sum_{m=1}^{M} \sum_{n=1}^{N} \|\hat{y}_{m,n} - y_{m,n}\| \tag{15}$$

$$RMSE = \left[\frac{1}{M \times N} \sum_{m=1}^{M} \sum_{n=1}^{N} \|\hat{y}_{m,n} - y_{m,n}\|^2 \right]^{\frac{1}{2}} \tag{16}$$

where $\hat{y}_{m,n}$ is the predicted average departure delay, $y_{m,n}$ is the actual value. M is the number of days in the test set, and N is the number intervals in each day.

3) Analysis of prediction results: We compare the prediction errors over the whole day. Figure 10 illustrates the delay prediction results for typical days at ATL. Within this figure, the prediction errors are represented by a confidence interval. It can be seen that the predicted value's overall trend is in line with the real value. Between 5 am and 6 am, the prediction error is the smallest, because there are a few delayed flights and it is easily to predict. The biggest prediction error is located between 8 am to 9 am. The main reason is that 8 am to 9 am is peak hours with much more random factors, which makes difficult for accurately prediction.

The performance results of the TDP-PPN model and baseline methods on the testing dataset are presented in Table II. Each experiment was independently repeated ten times, and the mean deviation is reported. Analysis of Table II yields the following observations: (a) TDP-PPN consistently demonstrates the superior performance across all statistical metrics at each prediction step, as evidenced by its smaller metric values compared to other models. (b) The accuracy of

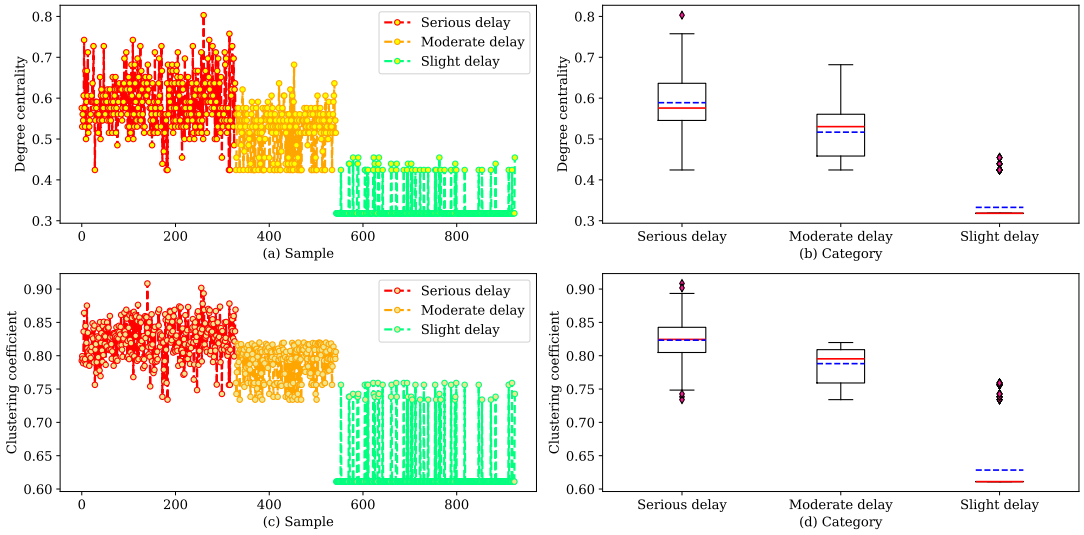

Fig. 9. The distribution of complex network characteristics under different delay levels

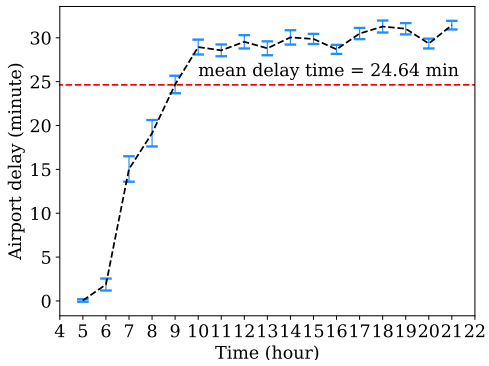

Fig. 10. Error bars of airport delay (ADD)

TABLE II
PARTIAL INDICATOR DATA PERFORMANCE COMPARISON OF DIFFERENT METHODS

Model	Metric	Hours			Mean
		1 h	2 h	3 h	
TDP-PPN	MAE	5.8095	6.0428	6.2	6.017433
	RMSE	8.5897	8.7599	9.1401	8.8299
XGBoost	MAE	5.766	8.673	9.365	7.935
	RMSE	9.652	13.17	14.422	12.415
DNN	MAE	6.371	7.193	7.614	7.059
	RMSE	9.796	10.344	10.524	10.221
LSTM	MAE	5.962	6.416	7.699	6.692
	RMSE	9.68	10.396	12.335	10.804

all prediction models tends to decrease as the prediction step increases, indicating heightened uncertainty associated with longer forecast periods. (c) In comparison to other models, the TDP-PPN model exhibits the slowest increase in prediction errors with an increase in the prediction step. At different prediction steps, TDP-PPN's MAE decreases by 2.56%, 5.82%, and 19.47% when compared to the LSTM model, respectively. This demonstrates the pronounced advantage of the TDP-PPN model with longer prediction steps.

4) Variant comparison: To further evaluate the performance of the proposed TDP-PPN model, we compare it with several variants. The TDP-PPN variants illustrated in the following, and their corresponding study results are presented in Table III:

- TDP-PPN-NN: A variant of TDP-PPN without considering complex network features.
- TDP-PPN-NP: A variant of TDP-PPN without considering daily and weekly periodicity.
- TDP-PPN-NW: A variant of TDP-PPN without considering weather impacts.
- TDP-PPN-NA: A variant of TDP-PPN with the attention mechanism module removed.

From Table III, the discoveries are as follows:

- Table III presents the performance of various models, and it is evident that TDP-PPN outperforms them all with the smallest MAE and RMSE. These results indicate that all four components of TDP-PPN collectively contribute to enhancing prediction accuracy.
- Across all prediction steps, TDP-PPN-NA consistently exhibits the highest MAE and RMSE among the five models, suggesting that the attention mechanism module plays a significant role in improving prediction performance.
- Except for TDP-PPN-NA, TDP-PPN-NN has the highest errors in 1-hour prediction. This reflects the importance of complex network features in short-term forecasting, and the topological characteristics of complex networks derived from time series data effectively capture the nonlinear dynamics of airport delays.
- Except for TDP-PPN-NA, TDP-PPN-NP has the highest errors in 3-hour prediction. This reflects the importance

TABLE III
RESULTS OF COMPARISON AMONG DIFFERENT VARIANTS IN TDP-PPN

M	Metrics	TDP-PPN-NN	TDP-PPN-NW	TDP-PPN-NP	TDP-PPN-NA	TDP-PPN
1 hour	MAE	5.8822	5.8560	5.8169	5.9441	5.8095
	RMSE	8.6570	8.6492	8.6188	8.6680	8.5897
2 hour	MAE	6.0990	6.1324	6.2017	6.2761	6.0428
	RMSE	8.8388	8.8750	8.9934	9.0293	8.7599
3 hour	MAE	6.2678	6.3279	6.3326	6.3599	6.2000
	RMSE	9.2042	9.4554	9.3690	9.4044	9.1401

of daily and weekly periodicity in long-term forecasting, as the airport delay time series has strong periodicity in long term.

VI. CONCLUSIONS

In this paper, we investigate the airport delay prediction problem from a novel perspective and develop a Temporal Convolution Networks (TCN) based airport Delay Prediction model considering local Proximity, global Periodicity and short-term Nonlinearity (TDP-PPN). Specifically, the complex network (converted from airport delay time series using Limited Penetrable Visibility Graph (LPVG) method) features within the airport delay time series are excavated and employed in TDP-PPN. Moreover, a three-channel TCN is embedded into the proposed approach to better learn the long-term and short-term characteristics of delay evolution simultaneously. Using operational data obtained from U.S. Department of Transportation, the proposed model is compared with several benchmark approaches in a study case involving about 40,0000 flights in ATL in 2019. The results show that our model outperforms the state-of-the-art baselines. Additionally, we evaluate the performances of TDP-PPN and its variants, and the results demonstrate the effectiveness of the components incorporated in our model.

In future work, we plan to investigate the incorporation of additional complex network features, including k-shell value and structure entropy, and explore the integration of complex network theory with other deep learning techniques, such as Gated Recurrent Units (GRUs) and Graph Convolutional Networks (GCNs), to enhance prediction accuracy. Moreover, we intend to incorporate other critical auxiliary features, such as airway weather and air traffic control information, into our model.

REFERENCES

[1] Civil Aviation Administration of China (2019) Bulletin on the Development of the Civil Aviation Industry in 2019. https://www.caac.gov.cn/

[2] EUROCONTROL (2020) Annual Network Operations Report 2019. https://www.eurocontrol.int/publication/annual-network-operations-report-2019

[3] United States Department of Transportation (2020) Bureau of Transportation Statistics, Airline Service Quality Performance. https://transtats.bts.gov/

[4] S. M. Li, D. F. Xie, X. Zhang, Z. Y. Zhang, and W. Bai, "Data-Driven Modeling of Systemic Air Traffic Delay Propagation: An Epidemic Model Approach", *Journal of advanced transportation*, vol. 2020, no. 6, pp. 1-12, 2020.

[5] Z. Yang, Y.x. Chen, J.b. Hu, Y.l.Song , Y. Mao. "Departure delay prediction and analysis based on node sequence data of ground support services for transit flights",*Transportation Research Part C:Emerging Technologies*, vol. 153, pp. 1-26, 2023.

[6] C. Li,J.F. Mao, L.Y. Li, J.X. Wu, L.M. Zhang, J.Y. Zhu, Z.B. Pan. "Flight delay propagation modeling: Data, Methods, and Future opportunities",*Transportation Research Part E: -LOGISTICS AND TRANSPORTATION REVIEW*, vol.185 ,pp.1-43 ,2024.DOI10.1016/j.tre.2024.103525.

[7] M. Chen, X. h. Yu, Y. Liu, "PCNN: Deep Convolutional Networks for Short-Term Traffic Congestion Prediction", *IEEE Transactions on Intelligent Transportation Systems*, vol. 19, no. 11, pp. 3550-3559, 2018.

[8] J. Zhang, M. Small, "Complex network from pseudo periodic time series: Topology versus dynamics", Physical review letters, vol. 96, no. 23, pp. 1-4,2006. https://doi.org/10.1103/PhysRevLett.96.238701

[9] P. Holme, J. Saramäki, "Temporal networks", Physics reports, vol. 519, no.3, pp: 97-125, 2012. https://doi.org/10.1016/j.physrep.2012.03.001.

[10] L. Lacasa, B. Luque, F. Ballesteros, J. Luque, J. C. Nuno, "From time series to complex networks: the visibility graph", Proceedings of the National Academy of Sciences of the United States of America, vol. 105, no, 13, pp: 4972-4975, 2008. https://doi.org/10.1073/pnas.0709247105.

[11] B. Luque, L. Lacasa, F. Ballesteros, J. Luque, "Horizontal visibility graphs: exact results for random time series", Physics Review E, vol,80,no,4, pp:1-11, 2009. https://doi.org/10.1103/PhysRevE.80.046103.

[12] Z. K. Gao, Q. Cai, Y.X. Yang, W. D. Dang, S. S. Zhang, "Multiscale limited penetrable horizontal visibility graph for analyzing nonlinear time series", Science Reports, vol. 6, pp: 1-7, 2016. https://doi.org/10.1038/srep35622.

[13] Y. Tu, M. O. Ball, and W. S. Jank, "Estimating flight departure delay distributions-a statistical approach with long-term trend and short-term pattern", *Journal of the American Statistical Association*, vol. 103, no. 481, pp. 112-125, 2008.

[14] E. R. Mueller, G. B. Chatterji, "Analysis of aircraft arrival and departure delay characteristics", in Pro. *AIAA's Aircraft Technology, Integration*, and Operations (ATIO), 2002, pp. 5866.

[15] S. Boswell, J. Evans, "Analysis of downstream impacts of air traffic delay", *Cambridge: Lincoln Laboratory, Massachusetts Institute of Technology*, 1997.

[16] J. T. Wong, S. C. Tsai, "A survival model for flight delay propagation", *Journal of Air Transport Management*, vol. 23, no. 7, pp. 5-11, 2012.

[17] M. Hansen, "Micro-level analysis of airport delay externalities using deterministic queuing models: a case study", *Journal of Air Transport Management*, vol. 8, no. 2, pp.73-87, 2002.

[18] N. Pyrgiotis, K. M. Malone, and A. Odoni, "Modelling delay propagation within an airport network", *Transportation Research Part C: Emerging Technologies*, vol. 27, pp. 60-75, 2013.

[19] P. Fleurquin, J. J. Ramasco, and V. M. Eguiluz, "Systemic delay propagation in the US airport network", *Scientific Report*, vol. 3, no. 1, pp. 1159, 2013.

[20] B. Baspinar, E. Koyuncu, "A Data-driven Air Transportation Delay Propagation Model using Epidemic Process Models", International Journal of Aerospace Engineering, vol. 11, pp. 1-11, 2016.

[21] F. Dai, P. G. Huang, Q. Mo, X. L. Xu, M. Bilal, and H. B. Song, "ST-InNet: Deep Spatio-Temporal Inception Networks for Traffic Flow Prediction in Smart Cities", *IEEE Transactions on Intelligent Transportation Systems*, vol. 23, no. 10, pp. 19782-19794, 2022.

[22] F. R. Huang, A. Jolfael, and A. K. Bashir, "Robust Multimodal Representation Learning with Evolutionary Adversarial Attention Networks", *IEEE Transactions on Evolutionary Computation*, vol. 25, no. 5, pp. 856-868, 2021.

[23] S. A. Rodríguez, F.G. Comendador, R. A. ValdéS, C. G. Perez, R. B. Montes, and S. C. Serrano, "Assessment of airport arrival congestion and delay: prediction and reliability", *Transportation Research Part C: Emerging Technologies*, vol. 98, pp. 255-283, 2019.

[24] G. Gui, F. Liu, J. L. Sun, J. Yang, Z. Q. Zhou, and D. X. Zhao, "Flight Delay Prediction Based on Aviation Big Data and Machine Learning",

IEEE Transactions on Vehicular Technology, vol. 69, no. 1, pp. 140-150, 2020.

[25] Y. J. Kim, S. Choi, S. Briceno, and D. Mavris, “A deep learning approach to flight delay prediction”. in: Pro. *IEEE/AIAA 35th Digital Avionics Systems Conference (DASC)*, 2016, pp. 1-6.

[26] W. L. Zeng, J. Li, Z. B. Quan, and X. B. Lu, “A Deep Graph-Embedded LSTM Neural Network Approach for Airport Delay Prediction”. Journal of Advanced Transportation, vol. 6638130, pp.1-15, 2021.

[27] H. Altaheri, G. Muhammad and M. Alsulaiman, ”Physics-Informed Attention Temporal Convolutional Network for EEG-Based Motor Imagery Classification,” in IEEE Transactions on Industrial Informatics, vol. 19, no. 2, pp. 2249-2258,2023.doi: 10.1109/TII.2022.3197419.

[28] S.J. Liu,T. Xu,X.Z. Du ,Y.C. Zhang,J.B. Wu, ”A hybrid deep learning model based on parallel architecture TCN-LSTM with Savitzky-Golay filter for wind power prediction”,vol. 302, no. 118122, pp. 1-20, 2024.https://doi.org/10.1016/j.enconman.2024.118122.

Shanmei Li received the B.E. degree from Beijing Jiaotong University, Beijing, China, in 2005, the M.E. degree from Jilin University, Changchun, China, in 2007, and the Ph.D. degree from Tianjin University, Tianjin, China, in 2014. She is currently an Associate Professor with the College of Air Traffic Management, Civil Aviation University of China. Her research interests include air traffic flow theory, complex network and data mining.

Dengjiang Sun received the B.S. degree in traffic and transportation from Civil Aviation University of China, Tianjin, China, in 2022. He is currently pursuing the M.S. degree in traffic and transportation planning and management with Beijing Jiaotong University. His research interests include intelligent transportation system, traffic flow modeling, connected and automated vehicles, and platoon control.

Chao Wang received the B.E. degree from Nanjing University of Aeronautics and Astronautics in 1995, the M.S. degree from Tianjin University in 2003, and the Ph.D. degree from Nanjing University of Aeronautics and Astronautics in 2012. He is currently a Professor with the College of Air Traffic Management, Civil Aviation University of China. His general areas of interest are air traffic control and air traffic simulation.

Siying Xu received the B.E. degree from Beijing Jiaotong University, Beijing, China, in 2005, the M.E. degree from Civil Aviation University of China, Tianjin, China, in 2008. She is with the Operation Supervisory Centre, Civil Aviation Administration of China, Beijing 100710, China. Her research interests include air traffic flow management and data mining.

Yang Yang is currently pursuing the bachelor’s degree with the Civil Aviation University of China, Tianjin, China. His research interests include air traffic control and intelligent transportation systems.

Xiaochun Cheng (*Senior Member, IEEE*) received the B.Eng. degree in computer engineering in 1992 and the Ph.D. degree in computer science in 1996. He has been working with U.K. University since 1997. One project was funded with 16 million Euro. He has contributed to five times the best conference paper awards so far. Five of his papers were in the top 1% of the academic field by data from Essential Science Indicators. He won three national competitions. He won the National Award. He contributed to two computer solutions, which achieved national best results and were adopted nationally.